

Photosynthetic capacity exhibits diurnal variation, implications for terrestrial biosphere models and gas exchange measurements

Joseph Stinziano¹, Marissa Harjoe¹, Cassandra Roback¹, Nellie Toliver¹, Alistair Rogers², and David T. Hanson³

¹University of New Mexico

²Brookhaven National Laboratory

³Affiliation not available

September 28, 2020

Abstract

Terrestrial biosphere models (TBMs) are extremely sensitive to the parameterization of the Farquhar, von Caemmerer & Berry model of photosynthesis, particularly the apparent maximum carboxylation capacity (V_{cmax}) of Rubisco. New instrumentation and approaches have enabled the rapid measurement of apparent V_{cmax} that paves the way for the investigation of diurnal variation in V_{cmax} and improved understanding of the potential impact on representation of photosynthesis in TBMs. Here we show that reductions in V_{cmax} over the course of a photoperiod can be as great as 50% and, when incorporated into a model of daily CO₂ assimilation, show that net carbon gain can change between -19 and 215% when compared to the current TBM assumption of a constant V_{cmax} . Given the obvious impact on TBM representation of photosynthesis, we recommend a renewed focus on the measurement of diurnal responses in photosynthetic capacity across biomes to advance understanding and enable model representation of this important phenomenon.

Introduction

Uncertainty in Earth system model projections of our future climate is largely driven by a lack of understanding and model representation of ecosystem processes associated with CO₂ assimilation and storage by the terrestrial biosphere (Friedlingstein *et al.* , 2014; Lovenduski & Bonan, 2017). Photosynthesis is the largest carbon flux on the planet and the gatekeeper process for an uncertain terrestrial carbon sink (Le Quere *et al.* , 2016). Terrestrial biosphere models (TBMs) are particularly sensitive to structural and parametric representation of photosynthesis (Friend, 2010; Bonan *et al.* , 2011; LeBauer *et al.* , 2013; Rogers, 2014; Sargsyan *et al.* , 2014; Rogers *et al.* , 2017; Ricciuto *et al.* , 2018). Photosynthetic capacity, specifically the apparent maximum carboxylation capacity of Rubisco at 25 °C ($V_{cmax,25}$), is a key model input that drives considerable uncertainty in TBM projections (Friend, 2010; Bonan *et al.* , 2011; LeBauer *et al.* , 2013; Sargsyan *et al.* , 2014). $V_{cmax,25}$ is further used to derive the maximum rate of electron transport (J_{max}), the triose phosphate utilization rate (when implemented) and respiration (R) (e.g. Sitch *et al.* , 2003; Rogers *et al.* , 2014; Lombardozzi *et al.* , 2018). If this key parameter shows significant diurnal variation, the implications for TBM projections of CO₂ assimilation could be notable.

Terrestrial biosphere models (TBMs) typically represent V_{cmax} as a fixed parameter (Rogers, 2014) but with some consideration of other factors such as day length (Bauerle *et al.* , 2012), temperature acclimation (Kattge & Knorr, 2007; Lombardozzi *et al.* , 2015; Smith *et al.* , 2015), and emerging potential for covariation with environmental drivers (Ali *et al.* , 2015; Smith *et al.* 2019). Only a few studies have investigated diurnal variation in V_{cmax} (Singsaas *et al.* , 2000; Kets *et al.* , 2010; Nascimento & Marenco, 2013). *In vitro*, Rubisco activation state changes rapidly with irradiance (Salvucci & Anderson, 1987; Parry *et al.* , 1997), shows

diurnal variation (Sage *et al.* , 1993; Pérez *et al.* , 2005), and is subject to regulation by Rubisco activase (Portis, 2003; Sage *et al.* , 2008), which could contribute substantially to diurnal variations in V_{cmax} . However, *in vitro* and *in vivo* data on Rubisco activation state can vary markedly (Rogers *et al.* , 2001; Sharwood *et al.* , 2017), and without an easy way to assess activation state *in vivo* , and an approach to incorporate *in vitro* measurements into TBM formulations, a gas exchange approach to measuring Rubisco activity is desirable.

While there is a paucity of data on whether diurnal changes in V_{cmax} occur (see Singaas *et al.* , 2000; Kets *et al.* , 2010; and Nascimento & Marengo, 2013 for examples), there are many studies investigating diurnal and circadian patterns in gas exchange parameters. Net CO₂ assimilation (A_{net}) is known to vary diurnally (Leverenz, 1981; Epron *et al.* , 1992; Singaas *et al.* , 2000; Panek, 2004; Leakey *et al.* , 2004; Harrison *et al.* , 2010; Kets *et al.* , 2010; Nascimento & Marengo, 2013; Bader *et al.* , 2016), which can be driven by environmental changes. There is a midday depression in net CO₂ assimilation that has been related to vapor pressure deficit and water relations (Tenhunen *et al.* , 1984; Rodà, 1999), whereby stomatal conductance mediates a supply-driven change in carbon assimilation (Leverenz, 1981; Epron *et al.* , 1992; Harrison *et al.* , 2010; Resco de Dios *et al.* , 2016a,b) and balances the need to fix carbon with preventing water loss (Matthews *et al.* , 2017), although circadian changes in A_{net} and g_s are decoupled from one another (Dodd *et al.* , 2004; Resco de Dios, 2017). Brodribb & Holbrook (2004) found that leaf hydraulic conductance declines over the day, which may mediate declines in mesophyll conductance (g_m) (Bickford *et al.* , 2009; Flexas *et al.* , 2013), reducing chloroplastic CO₂ supply (and therefore A_{net}) later in the day and may even mediate changes in stomatal behaviour (Sack *et al.* , 2016). Nardini *et al.* . (2005) found that leaf hydraulic conductance (K_{leaf}) was under circadian regulation in *Helianthus annuus* , which was the cause of diurnal oscillations in K_{leaf} . There may be further changes in realized quantum yield of photosynthesis that result from delays in recovering from photoprotection or photodamage throughout the day, limiting energy available for carbon fixation (Long & Humphries, 1994; Gamon, 2015; Kromdijk *et al.* , 2016). As well, there are diurnal shifts in carbohydrate accumulation, and this can lead to feedback inhibition of photosynthesis (Sun *et al.* , 1999). In this way, diurnal changes in net CO₂ assimilation can be driven by both supply and demand of substrates, and these diurnal changes in gas exchange scale up to the canopy level (Resco de Dios, 2016a). Many of the diurnal changes in A_{net} outlined above are due to diurnal environmental changes which models can mimic well. However, it is unclear whether there may be diurnal variation in V_{cmax} , and if there is, diurnal variation in V_{cmax} may present a simple way to account for the effect of diurnal changes in leaf carbon exchange in models.

Current approaches for measuring V_{cmax} *in vivo* require measurement of the response of photosynthesis (A) to internal CO₂ concentration (C_i) which can take over an hour for a single measurement (Bernacchi *et al.* , 2003). Recently, Stinziano *et al.* . (2017) developed a method for the rapid measurement of the $A-C_i$ response (the RACiR technique). The dramatic shortening of measurement time enables the collection of high-resolution diurnal patterns in apparent V_{cmax} and apparent J_{max} (Stinziano *et al.* , 2017, 2019ab; Coursolle *et al.* , 2019; Lawrence *et al.* , 2019). In addition, this new technique provides values for parameters measured *in vivo* that are directly applicable to current TBM model formulations and enables measurement of diurnal dynamics under circumstances where *in vitro* work cannot be done, e.g. where sampling constraints in remote locations are logistically challenging, or when secondary compounds limit the ability to successfully extract and measure Rubisco activity. Studies assessing TBM performance on a diurnal scale are limited (in some cases due to temporal resolution of the models). in the case of ORCHIDEE, carbon fluxes are consistently over-estimated relative to eddy covariance data later in the day across plant functional types (Krinner *et al.* , 2005), while the Community Atmosphere Model (CAM4 and CAM5) over-estimates latent heat fluxes later in the day at mid-latitude and boreal regions (Lindvall *et al.* , 2012) suggesting an over-estimation of transpiration, which would imply overestimations of stomatal conductance, C_i , and A_{net} . These discrepancies may be related to endogenous rhythms in ecosystem-level gas exchange (Resco de Dios *et al.* , 2012) that are currently unaccounted for.

Our objective was to determine whether diurnal variation in V_{cmax} occurs, and if so, the extent to which such variation affects leaf-level gas exchange modeling. Here we show that the RACiR technique can be used to

successfully measure diurnal variation in V_{cmax} . We demonstrate that diurnal variation in V_{cmax} is variable across 11 species from several plant functional types, leading to a variable effect on modelled leaf-level gas exchange, underscoring the need to consider diurnal dynamics in V_{cmax} when modeling.

Materials and Methods

Plant Material

Cuttings of poplar (*Populus deltoides* Barr. S7c8 East Texas day neutral clone; and *Populus trichocarpa* BESC2074639) were grown at the University of New Mexico (35.0843° N, 106.6198° W, 1587 m a.s.l.) at 18.3 to 21.1/15.6 to 21.1 °C day/night temperature in a rooftop greenhouse, and bell pepper (*Capsicum annuum* var. V6220 California Wonder Bell Pepper) were grown in an indoor greenhouse at 22/16 °C day/night temperature with 12/12 day/night photoperiod maintained using a SPYDR 600 LED lighting system (BML Horticulture, Austin, TX, USA) at a minimum intensity of 170 $\mu\text{mol m}^{-2} \text{s}^{-1}$ (maximum light intensity of $\sim 720 \mu\text{mol m}^{-2} \text{s}^{-1}$ including the natural light in the indoor greenhouse). *Populus deltoides* were grown in 28 L pots and were ~ 2 years old during measurements, *Populus trichocarpa* were grown in 7 L pots and were < 6 months old during measurements, and *Capsicum annuum* were grown in 28 L pots. All three greenhouse species were grown in Metro-Mix 300 potting soil (Sun Gro Horticulture, Seba Beach, AB, Canada), and were fertilized twice weekly with Peters 20-20-20 (Scotts Miracle-Gro, Marysville, OH, USA) and once weekly with chelated liquid iron (Ferti-Lome, Bonham, TX, USA). USDA-certified organic Granny Smith apple trees (*Malus domestica* Borkh.) were grown in Los Lunas, NM at the New Mexico State University Agricultural Science Center (34.6007° N, 103.2139° W, 1793 m a.s.l., MAP: 241 mm, MAT: 13.9 °C, Soil: loam, Slope: 0 – 1%; USDA, 2018). Showy milkweed (*Asclepias speciosa*), mature Chinquapin oak (*Quercus muehlenbergii*), and Queen Elizabeth rose (*Rosa grandiflora*) were grown at the ABQ BioPark Botanic Garden in Albuquerque, NM (35.0933° N 106.6813° W, 1587 m a.s.l., MAP: 203 mm, MAT: 17.5 °C, Soil: fine sandy loam, Slope: 0 – 1%, USDA, 2018). Mature ponderosa pine (*Pinus ponderosa*) were measured at Las Huertas Upper Picnic Grounds in Cibola National Forest, Sandoval County, NM (35.235458° N, 106.413012° W, 2316 m a.s.l., MAP: 546 mm, MAT: 6.1 °C, Soil: stony loam, Slope: 35 – 70%, USDA, 2018). Measurements were made on October 26th, 2017, and observed sunrise/sunset was 8:30am and 5:00pm due to the location of the measurement site in a canyon with mountains on all sides. Mature Deodar cedar (*Cedrus deodar*, sample size limited to 4 available trees) and mature ginkgo (*Ginkgo biloba*, sample size limited to 3 available trees) from the University of New Mexico Arboretum (35.0843° N, 106.6198° W, 1587 m a.s.l., MAP: 203 mm, MAT: 17.5 °C, Soil: cut and fill, USDA, 2018) were measured on August 24th, 2018. Unless stated above, sample size for each species was one leaf (or branch for needleleaf species) from each of six individuals. Note: the timing of measurements and sample size varied depending on access to equipment, facilities and biological material (especially for field measurements), however this should not affect the presence or absence of diurnal changes in V_{cmax} .

Gas exchange measurements

The RACiR technique was used according to Stinziano *et al.* (2017, 2019a). Briefly, we used a Licor 6800 portable photosynthesis machine equipped with a fluorescence head (Licor Biosciences, Lincoln, Nebraska, USA), and tailored chamber and RACiR parameters to each species (Table 1). RACiR range was selected after initial analyses to ensure that we captured part of the inflection region of the $A-C_i$ response as required by the curve fitting procedure we used. Initial light responses were measured to determine saturating light intensity for each species. Note that the overpressure (ΔP) controls and accounts for chamber leaks. Starting at Zeitgeber Time (ZT, also photoperiod time; the time since sunrise) of 1 hour (1 hour after meteorological sunrise) on October 31st, 2016, RACiR curves were run every hour until ZT10 for *Populus deltoides*, while for *Populus trichocarpa*, RACiR curves were run on November 30th, 2016 every 1.5 hours from ZT1.5 until ZT9. For *Capsicum annuum*, RACiR curves were run every two hours from ZT0 until ZT12. *Malus domestica* were measured in the field every two hours from ZT2.5 until ZT8.5 on October 9th, 2016. *Asclepias speciosa*, *Quercus muehlenbergii*, and *Rosa grandiflora* were measured on June 28th, 2018 from \sim ZT1.5 until \sim ZT12. *Pinus ponderosa* were measured on October 26th, 2017 from observed \sim ZT0.5 to \sim ZT8.5 (meteorological ZT1.5 to ZT9.5). Due to issues with low g_s (which can interfere with C_i calculations), sample size for each

time point for *P. ponderosa* varies from 1 to 4. *Cedrus deodar* and *Ginkgo biloba* were measured from ZT2.5 until ZT12 on August 24th, 2018. All measurements were performed on the same area of leaf tissue for broad leaf species and the same branch for each needle leaf species. Note that due to external environmental temperatures, *Asclepias speciosa*, *Quercus muehlenbergii*, *Rosa grandiflora*, *Cedrus deodar*, and *Ginkgo biloba* were all measured at 30 °C. Dark respiration (R) was measured in each species by letting the leaf equilibrate to dark cuvette conditions for 30 min prior to measurements (note: chamber conditions are outlined in Table 1).

RACiR data were corrected using the R package {racir} (Stinziano, 2018) and were analyzed for V_{cmax} and J_{max} using the {plantecophys} package (Duursma, 2015) in R v3.5.1 (R Core Team, 2018), and default parameters were used as in Stinziano *et al.* (2017), which correspond to Rubisco kinetics and thermal coefficients as in Bernacchi *et al.* (2001).

Clamping Experiment

We tested the impacts of repeated clamping on leaves of *Capsicum annuum*, *Populus deltoides*, and *Populus trichocarpa*. For each of five sequential clamps on each measured leaf, we allowed the chamber to stabilize (< 2 min in all cases), and measured A_{net} at 400 $\mu\text{mol CO}_2\text{mol}^{-1}$ for 30 s at 0.5 Hz. Between clamps, the leaf was given a 1 min recovery. On clamps 1 and 5, a RACiR was run as specified above for each species. We then fit V_{cmax} and J_{max} as above. These measurements were performed on an individual leaf spot within 30 min to minimize diurnal effects.

Modeling A_{net}

We modelled photosynthesis according to Farquhar *et al.* (1980), where A_{net} is the minimum of carboxylation and electron transport limitations:

$$A_{net} = \min(A_c, A_j, A_t) - R_d \text{ (Equation 1)}$$

$$A_c = V_{c,max} \frac{C_i - \Gamma^*}{C_i + K_c \left(1 + \frac{O}{K_o}\right)} \text{ (Equation 2)}$$

$$A_j = J \frac{(C_i - \Gamma^*)}{4C_i + 8\Gamma^*} \text{ (Equation 3)}$$

$$[J - 0.5(1 - f)I][J - J_{max}] = 0 \text{ (Equation 4)}$$

$$A_t = V_{c,max}/2 \text{ (Equation 5)}$$

Where A_c , A_j , and A_t are carboxylation, electron transport, and triose phosphate utilization limited photosynthesis, respectively; R_d is respiration in the light; $V_{c,max}$ is the maximum rate of Rubisco carboxylation, C_i is leaf intercellular [CO_2]; Γ^* is the CO_2 compensation point in the absence of mitochondrial respiration; K_c and K_o are the Michaelis-Menten constants for Rubisco carboxylation and oxygenation, respectively; O is the O_2 concentration in the chloroplast ($O = 210 \mu\text{mol mol}^{-1}$); J is the rate of photosynthetic electron transport; f is the fraction of light energy not absorbed by the chloroplast (0.15); I is the incident irradiance; and J_{max} is the maximum rate of photosynthetic electron transport.

$V_{c,max}$, J_{max} , K_c , K_o , and Γ^* were thermally scaled using an Arrhenius equation:

$$f(T) = k_{ref} \exp \left[E_a \frac{T - T_{ref}}{T \times T_{ref} \times R_g} \right] \text{ (Equation 6)}$$

Where $f(T)$ is the parameter at temperature T in K; k_{ref} is the parameter at the reference temperature (either 25 °C or 30 °C); T_{ref} is the reference temperature in K (either 298 K or 303 K); E_a is the activation energy in kJ mol^{-1} ; and R_g is the universal gas constant ($0.008314 \text{ kJ K}^{-1}\text{mol}^{-1}$). See Bernacchi *et al.* (2001) for E_a , and k_{ref} for all parameters except J_{max} , and see Bernacchi *et al.* (2003) for E_a for J_{max} (note that k_{ref} for $V_{c,max}$ and J_{max} were derived from measured RACiR curves for each species).

Respiration (R) was modelled as according to Atkin & Tjoelker (2003):

$$f(T) = 10^{\frac{T - T_{ref}}{10} \times Q_{10} + R_{ref}} \text{ (Equation 7)}$$

Where $f(T)$ is the parameter at temperature T in K; Q_{10} is the thermal sensitivity coefficient (assumed to be 2); and R_{ref} is respiration at the reference temperature.

Since the photosynthetic rates depend on C_i , we modelled CO_2 diffusion into the leaf using Moss and Rawlins (1963):

$$A_{net} = g_s (C_a - C_i) \text{ (Equation 8)}$$

Where g_s is stomatal conductance ($\text{mol m}^{-2} \text{ s}^{-1}$), C_a and C_i are the concentrations of CO_2 at the leaf surface and intercellular airspace, respectively ($\mu\text{mol mol}^{-1}$).

To close the system of equations, we used the stomatal conductance model from Medlyn *et al.* (2011) as implemented by Lin *et al.* (2015):

$$g_s = 1.6 \left(1 + \frac{g_1}{\sqrt{D}} \right) \frac{A_{net}}{C_a} \text{ (Equation 9)}$$

Where g_1 is the model coefficient equal to 4.16, and D is vapor pressure deficit.

Daily net leaf carbon uptake was modelled in R assuming an ambient CO_2 concentration (C_a) of $400 \mu\text{mol mol}^{-1}$, and constant dark respiration (R) at 25°C (unless otherwise stated) ($2.27 \pm 0.16 \mu\text{mol m}^{-2} \text{ s}^{-1}$ for *Populus deltoides*, $0.46 \pm 0.15 \mu\text{mol m}^{-2} \text{ s}^{-1}$ for *Capsicum annuum*, $3.36 \mu\text{mol m}^{-2} \text{ s}^{-1}$ for *Malus domestica* (Bunce, 1992), $2.30 \pm 0.16 \mu\text{mol m}^{-2} \text{ s}^{-1}$ for *Populus trichocarpa*, $2.49 \pm 1.00 \mu\text{mol m}^{-2} \text{ s}^{-1}$ for *Asclepias speciosa* (30°C), $0.74 \pm 0.07 \mu\text{mol m}^{-2} \text{ s}^{-1}$ for *Quercus muehlenbergii* (30°C), $1.85 \pm 1.08 \mu\text{mol m}^{-2} \text{ s}^{-1}$ for *Rosa grandiflora* (30°C), $0.24 \mu\text{mol m}^{-2} \text{ s}^{-1}$ for *Pinus ponderosa* (10°C ; Law *et al.*, 2001), $0.71 \pm 0.11 \mu\text{mol m}^{-2} \text{ s}^{-1}$ for *Ginkgo biloba* (30°C), and $0.85 \pm 0.22 \mu\text{mol m}^{-2} \text{ s}^{-1}$ for *Cedrus deodar* (30°C)). Environmental conditions at the University of New Mexico were taken for June 28, August 24, and October 9 in 2018 (Fig. 1) and used to provide driving data for all species. Half-hourly time intervals were summed for total carbon uptake for all species. Models were run for four scenarios (1) V_{cmax} and J_{max} scaled from maximum V_{cmax} and J_{max} to account for diurnal dynamics, (2) maximum measured V_{cmax} and J_{max} , (3) minimum measured V_{cmax} and J_{max} , and (4) average measured V_{cmax} and J_{max} . All R code is available as a supplementary file (“Stinziano et al Modeling.Rmd”, “environmentdata.csv”). We also tested the diurnal modeling by modeling the leaf chamber conditions used to measure RACiR at each time point for each species, comparing modelled A_{net} and g_s at $400 \mu\text{mol CO}_2 \text{ mol}^{-1}$. We then tested model performance by using the {lm} function in R (R Core Team, 2018).

Data analysis

Zeitgeber Time 0 (ZT0) was calculated based on meteorological sunrise ($07:30$ for *Populus deltoides* and *Populus trichocarpa*; $07:00$ for *Malus domestica*; $06:00$ for *Asclepias speciosa*, *Quercus muehlenbergii*, and *Rosa grandiflora*; $06:30$ for *Ginkgo biloba* and *Cedrus deodar*), observed sunrise for *Pinus ponderosa* ($08:30$) or the time that growth lights turned on ($08:30$ for *Capsicum annuum*). Diurnal variation was tested within each species using a repeated measures linear regression using the {lme} function of the {nlme} package in R (Pinheiro *et al.*, 2018). Relative $V_{c,max}$ and J_{max} were calculated for each species by standardizing to the highest average value (i.e. dividing $V_{c,max}$ and J_{max} at each time point by the peak $V_{c,max}$ and J_{max}) within a species.

Results

Photosynthetic capacity shows diurnal variability

Photosynthetic capacity (both V_{cmax} and J_{max}) at 25°C shows significant diurnal change with a consistent decline of $\sim 50\%$ towards the end of day, with the largest declines beginning at ZT8 in *Populus deltoides* (2^{nd} order polynomial responses; $V_{cmax} : t_{52} = -6.67, P < 0.0001$; $J_{max} : t_{52} = -7.30, P < 0.0001$; Fig. 2a, d), ZT8 in *Capsicum annuum* ($V_{cmax} : t_{33} = -5.24, P < 0.0001$; $J_{max} : t_{33} = -4.10, P = 0.0003$; Fig. 2b, e), and ZT2 in *Malus domestica* ($V_{cmax} : t_{17} = -9.25, P < 0.0001$); $J_{max} : t_{17} = -9.13, P < 0.0001$; Fig. 2b, e). *Populus trichocarpa* showed slight but significant declines in V_{cmax} at 25°C ($t_{19} = -3.39, P = 0.003$) and J_{max} ($t_{19} = -2.81, P = 0.01$) (Fig. 2b, e). *Pinus ponderosa* did not show any significant declines in V_{cmax} ($t_8 = -1.50, P =$

0.17) or J_{max} ($t_8 = -1.71$, $P = 0.13$; Fig. 2c, f). Photosynthetic capacity measured at 30 °C shows significant diurnal changes in V_{cmax} for *Quercus muehlenbergii* ($t_{24} = -6.39$, $P < 0.0001$; Fig. 2a), *Rosa grandiflora* ($t_{24} = -5.57$, $P < 0.0001$, Fig. 2b), and *Ginkgo biloba* ($t_{14} = -5.90$, $P < 0.0001$; Fig. 2c) but not *Asclepias speciosa* ($t_{24} = -1.77$, $P = 0.09$; Fig. 2a) and *Cedrus deodar* ($t_{20} = 0.648$, $P = 0.52$; Fig. 2c). For J_{max} at 30 °C, there are linear declines in *Quercus muehlenbergii* ($t_{24} = -5.75$, $P < 0.0001$; Fig. 2d), *Rosa grandiflora* ($t_{24} = -5.95$, $P < 0.0001$; Fig. 2e), *Ginkgo biloba* ($t_{14} = -9.29$, $P < 0.0001$; Fig. 2f) and *Asclepias speciosa* ($t_{24} = -2.09$, $P = 0.047$; Fig. 2d), but not for *Cedrus deodar* ($t_{20} = -0.10$, $P = 0.92$; Fig. 2f). Across all species, apparent J_{max} and V_{cmax} were strongly correlated as expected (slope = 1.99, intercept = -13.54, $F_{1,293} = 1826$, $R^2 = 0.86$, $P < 0.0001$; Fig. 3; Wullschleger, 1993). Diurnal variation in relative photosynthetic capacity is quite variable (Fig. 4), with convergent responses for *Capsicum annuum*, *Ginkgo biloba*, *Malus domestica*, and *Rosa grandiflora*, but varying patterns in the remaining species.

Modeling diurnal A_{net} responses

Using the species-specific diurnal patterns (Fig. 2), we modelled A_{net} for all species with diurnal changes in V_{cmax} and J_{max} (scaled to maximum average V_{cmax} and J_{max}), maximum (peak) V_{cmax} and J_{max} , average V_{cmax} and J_{max} , and minimum V_{cmax} and J_{max} (Fig. 5). When integrating modelled A_{net} over three separate 24-hour periods, accumulated net carbon gain is increased under peak photosynthetic capacity relative to the diurnal case by ~8 to 215% (corresponding to a 5 to 67% change in gross CO₂ assimilation (A_{gross}); Table 2, Fig. 5). Under average photosynthetic capacity relative to the diurnal case, A_{net} changes by -19 to 36% (corresponding to a -16 to 28% change in A_{gross} ; Table 2, Fig. 5). Under minimum photosynthetic capacity relative to the diurnal case, A_{net} changes by -303 to -6% (corresponding to a -61 to -4% change in A_{gross} ; Table 2, Fig. 5).

Measurement and modeling bias assessment

To determine whether repeated clamping could bias the measurements (i.e. through leaf damage), we ran RA-CiRs after 1 and 5 one-minute clamps on the three greenhouse species (*Capsicum annuum*, *Populus deltoides*, and *Populus trichocarpa*). We found no significant decline between clamps 1 and 5 for V_{cmax} (*Capsicum annuum*: $t_2 = -1.47$, $P = 0.28$; *Populus deltoides*: $t_4 = -1.82$, $P = 0.14$; *Populus trichocarpa*: $t_5 = -1.67$, $P = 0.16$; Fig. 6a), J_{max} (*Capsicum annuum*: $t_2 = -1.43$, $P = 0.29$; *Populus deltoides*: $t_4 = -2.01$, $P = 0.11$; *Populus trichocarpa*: $t_5 = -1.70$, $P = 0.15$; Fig. 6b), and A_{net} (*Capsicum annuum*: $t_2 = 1.39$, $P = 0.40$; *Populus deltoides*: $t_4 = -1.84$, $P = 0.21$; *Populus trichocarpa*: $t_2 = 0.48$, $P = 0.68$; Fig. 6c).

To check for model biases, we compared model predictions of the leaf-level gas exchange to measured A_{net} and g_s . The model consistently over-estimated A_{net} by 9.8% (slope = 1.098, $R^2 = 0.96$, $F_{1,63} = 1356$, $P < 0.0001$) while underestimating g_s by ~18% (slope = 0.82, $R^2 = 0.85$, $F_{1,63} = 345$, $P < 0.0001$) (Fig. 7).

Discussion

Apparent photosynthetic capacity exhibits substantial diurnal variation

There is substantial diurnal variation in apparent photosynthetic capacity (apparent V_{cmax} and J_{max}) (ranging from 0% change to over 50% decline). This variation has been ignored by TBMs, which typically use fixed estimates of apparent V_{cmax} and by leaf level physiologists who previously lacked an approach to collect high temporal resolution data *in vivo*. While we found interspecific differences in the diurnal response, the decline in apparent V_{cmax} and apparent J_{max} has important implications for modelling photosynthetic carbon uptake and should not be ignored.

Possible mechanisms for diurnal variation in photosynthetic capacity

We were able to rule out that repeated clamping could cause the substantial diurnal declines in photosynthetic capacity in the three species we tested (Fig. 6). Regarding biological mechanisms, the decline in apparent V_{cmax} could be driven by declines in Rubisco activation (Pérez *et al.*, 2005), diurnal changes in mesophyll conductance (Bickford *et al.*, 2010), diurnal changes in K_{leaf} (Brodribb & Holbrook, 2004), or possibly from the movement of chloroplasts (e.g. Tholen *et al.*, 2008). Rubisco activase is regulated by light through

ATP:ADP (Streusand & Portis, 1987) and redox potential (Zhang *et al.*, 2002), and is responsible for removing the inhibitor 2-carboxyarabinitol 1-phosphate (CA1P) from Rubisco (Robinson & Portis, 1988); therefore diurnal changes in irradiance may be regulating apparent V_{cmax} through changes in Rubisco activase activity. CA1P could be further implicated in diurnal regulation of apparent V_{cmax} , as it exhibits diurnal changes associated with changes in *in vitro* Rubisco activity in several species – though not all species have CA1P (Kobza & Seemann, 1989). Mesophyll conductance ultimately determines the supply of CO₂ from the intercellular airspace to the chloroplast, and diurnal changes in mesophyll conductance may cause changes in the slope of the $A-C_i$ response, leading to a false interpretation that there are diurnal changes in apparent V_{cmax} . Mesophyll conductance is tightly linked to K_{leaf} (leaf hydraulic conductance), which exhibits diurnal dynamics (Brodribb & Holbrook, 2004) which could then mediate diurnal changes in apparent V_{cmax} via mesophyll conductance (Flexas *et al.*, 2013). If we assume that the diurnal patterns observed in K_{leaf} are general, then declines in K_{leaf} would reduce g_m (Flexas *et al.*, 2013), reducing apparent V_{cmax} and J_{max} . However, these effects appear nonlinear, and we would have expected nonlinear diurnal dynamics, which we only observed in *P. deltooides*. Meanwhile, chloroplast movements (Tholen *et al.*, 2008) could also mediate changes in mesophyll conductance. We note that applying the model of Farquhar *et al.* (1980) in full, accounting for both mesophyll conductance and Rubisco activation state, could allow for V_{cmax} to remain constant while apparent V_{cmax} could vary diurnally. Whether such mechanisms explain diurnal dynamics in apparent V_{cmax} remains to be seen.

Model biases

The model tended to over-estimate A_{net} and under-estimate g_s , although the correlations between the measured and modelled data were quite strong ($R > 0.9$ for both) suggesting that our modeling correctly captured the behaviour of A_{net} and g_s . These biases have several possible sources: 1) the RACiR measurements were obtained as soon as the leaf chamber stabilized, which means that while the RACiR data may reflect the underlying biochemistry, the stomata will not have adjusted to the irradiance and the vapor pressure deficit in the leaf chamber that drives the Medlyn *et al.* (2011) stomatal conductance model. Since the modeling assumes a steady state, this could contribute to the biases. 2) RACiR is known to introduce metabolic mismatches that do not affect V_{cmax} and J_{max} estimates, but may affect A_{net} values (Stinziano *et al.*, 2019ab). These metabolic mismatches might thus contribute to some of the bias, although it should be minimal at the RACiR rates used (i.e. 100 $\mu\text{mol CO}_2 \text{ mol}^{-1} \text{ min}^{-1}$). 3) It is possible that respiration in the light is greater than respiration in the dark for some of these species. In this case, modelled A_{net} would necessarily over-estimate measurements of A_{net} . 4) We used the general slope from Lin *et al.* (2015) for the Medlyn *et al.* (2011) model. It is also possible that there is variation in the stomatal slope parameter (g_1) between species (Wolz *et al.* 2017; Miner *et al.* 2017; Franks *et al.* 2018).

Implications for measuring V_{cmax}

In terms of measuring V_{cmax} , the required timing of V_{cmax} measurements depends on the aims of the measurements. For comparing maximum apparent V_{cmax} , our data suggest that for most species, photosynthetic CO₂ responses should be measured in the morning, prior to midday. If the aim is to obtain data useful for model parameterization, there are two avenues: daily average or diurnal photosynthetic CO₂ response measurements. For daily average measurements, care is needed to make sure that the measurements occur across the entire light period of the photoperiod, with the recognition that there may be biases in conclusions based on average V_{cmax} . For diurnal measurements, there are again two approaches: RACiR, and the one-point method to estimating V_{cmax} . We have demonstrated this diurnal application of RACiR, however RACiR may not be feasible in all cases due to equipment or instrument precision. However, De Kauwe *et al.* (2016) showed that the one-point method for estimating apparent V_{cmax} can produce similar estimates to those from full photosynthetic CO₂ responses, providing sufficient time is allowed for leaf gas exchange to reach steady state in the chamber (Burnett *et al.* 2019). Given that diurnal dynamics in V_{cmax} can incur large changes on timescales of < 2 hrs, diurnal dynamics would affect temperature response measurements of V_{cmax} , with the effect dependent on which temperatures are measured earlier or later. It may be possible to circumvent these effects using RACiR-based approaches to temperature responses, although the timescales for chamber

equilibration times may limit such an approach. We call for more diurnal measurements of V_{cmax} as current measurement approaches may be introducing biases into conclusions based on the assumption the V_{cmax} is diurnally static.

Implications for TBMs

Accounting for diurnal dynamics of apparent V_{cmax} and J_{max} means that gross carbon assimilation could be mis-estimated ~-4 to 40% (standard deviation based on the average and peak V_{cmax} scenarios relative to the diurnal scenario). If extrapolated to global gross primary production (~123 Pg C yr⁻¹; Beer *et al.*, 2010), diurnal variation in photosynthetic parameters could create a revised estimate range of 101 ± 27 Pg C yr⁻¹ (mean \pm standard deviation) in global GPP. This uncertainty introduced here is similar to the uncertainty in unconstrained CMIP5 estimates of GPP (standard deviation: 27.5 Pg C yr⁻¹; Mystakidis *et al.*, 2016), implying that understanding diurnal processes regulating V_{cmax} may warrant more attention. Although limited in scope, this study clearly shows that diurnal variation in apparent V_{cmax} and J_{max} exists across multiple species under greenhouse and field conditions. While there are factors such as mesophyll conductance, K_{leaf} , and Rubisco activation state that could cause these diurnal dynamics in apparent V_{cmax} such that there is no effect on the amount of Rubisco in the leaf, it is important to note that TBMs currently use apparent V_{cmax} to model carbon assimilation (Rogers *et al.*, 2017). TBMs are also not ready for incorporation of g_m , Rubisco activation state, and K_{leaf} due to a paucity of data for these parameters. Therefore, if multiple processes are producing diurnal changes in apparent V_{cmax} , then including diurnal dynamics in apparent V_{cmax} may present a relatively simple way to include these important dynamics in TBMs. However, this requires broad diurnal RACiR surveys, paired with measurements such as g_m , Rubisco activation state, and K_{leaf} , to confirm the underlying mechanisms behind diurnal V_{cmax} .

Implementing diurnal changes in V_{cmax} into TBMs requires more physiological understanding of this phenomenon. Our data provide preliminary evidence that diurnal variation in V_{cmax} may depend on the evolutionary history of the organism as well (the two species from *Pinaceae* did not show a diurnal pattern), however this could be related to different diurnal dynamics (or lack thereof) in g_m , Rubisco activation state, and K_{leaf} . These areas still require a marked advance in process knowledge of g_m (Rogers *et al.*, 2017), Rubisco activation state, and K_{leaf} before they could be implemented into TBMs. However, ignoring these diurnal dynamics could lead to a mis-estimation of CO₂ assimilation by TBMs, especially since diurnal variation could be as significant as other sources of variation (e.g. leaf age, Wu *et al.*, 2016; species, Wullschleger, 1993; model structure, Mystakidis *et al.*, 2016). Greater mechanistic understanding of diurnal variation in V_{cmax} and quantification of the phenomenon in key biomes is required to so that improved model formulations of photosynthesis can be considered for inclusion in future TBMs.

Acknowledgments

We would like to thank Jeremiah Anderson, Kaitlyn Read, and Jun Tominaga for their help in the field, Mark Marsalis of the New Mexico State University Agricultural Center for allowing us to conduct research on their land, Todd Rosenstiel (Portland State University) for providing *P. deltoides*, David Weston (Oak Ridge National Lab) for providing *P. trichocarpa*, and Maria J. Thomas (ABQ BioPark Botanic Gardens) for allowing us to conduct research at the botanical gardens. This research was partially supported by a Fulbright Canada scholarship to JRS. JRS would also like to acknowledge scholarship support from the Natural Sciences and Engineering Research Council of Canada (NSERC). This work was also supported by funding to DTH through the NSF EPSCoR Program under Award # IIA-1301346 at the University of New Mexico. Any opinions, findings, and conclusions or recommendations expressed in this material are those of the authors and do not necessarily reflect the views of the National Science Foundation. AR was supported by the Next-Generation Ecosystem Experiments (NGEE Arctic and NGEE Tropics) projects that are supported by the Office of Biological and Environmental Research in the Department of Energy, Office of Science, and through the United States Department of Energy contract No. DE-SC00112704 to Brookhaven National Laboratory.

Author Contributions

JRS, MJH, CR, and NLT carried out the research. JRS and DTH designed the study. All authors contributed ideas and provided written input. JRS wrote the manuscript with input from all authors.

References

- Ali AA, Xu CG, Rogers A, McDowell NG, Medlyn BE, Fisher RA, Wullschleger SD, Reich PB, Vrugt JA, Bauerle WL *et al.* 2015. Global-scale environmental control of plant photosynthetic capacity. *Ecological Applications* **25** : 2349–2365.
- Bader MK-F, Mildner M, Baumann C, Leuzinger S, Körner C . 2016 . Photosynthetic enhancement and diurnal stem and soil carbon fluxes in a mature Norway spruce stand under elevated CO₂. *Environmental and Experimental Botany* **124** : 110–119.
- Bauerle WL, Oren R, Way DA, Qian SS, Stoy PC, Thornton PE, Bowden JD, Hoffman FM, Reynolds RF .2012 . Photoperiodic regulation of the seasonal pattern of photosynthetic capacity and the implications for carbon cycling. *Proceedings of the National Academy of Sciences of the United States of America* **109** : 8612–8617.
- Beer C, Reichstein M, Tomelleri E, Ciais P, Jung M, Carvalhais N, Rödenbeck C, *et al.* . 2010 . Terrestrial gross carbon dioxide uptake: global distribution and covariation with climate. *Science Express* **1184984** .
- Bernacchi CJ, Singaas EL, Pimentel C, Portis Jr. AR, Long SP. 2001. Improved temperature response functions for models of Rubisco-limited photosynthesis. *Plant, Cell & Environment* **24** : 253–259.
- Bernacchi CJ, Pimentel C, Long SP. 2003. *In vivo* temperature response functions of parameters required to model RuBP-limited photosynthesis. *Plant, Cell & Environment* **26** : 1419–1430.
- Bickford CP, McDowell NG, Erhardt EB, Hanson DT . 2009 . High-frequency field measurements of diurnal carbon isotope discrimination and internal conductance in a semi-arid species, *Juniperus monosperma* . *Plant, Cell & Environment* **32** : 796–810.
- Bickford CP, Hanson DT, McDowell NG. 2010. Influence of diurnal variation in mesophyll conductance on modelled ¹³C discrimination: results from a field study. *Journal of Experimental Botany* **61** :3223–3233.
- Bonan GB, Lawrence PJ, Oleson KW, Levis S, Jung M, Reichstein M, Lawrence DM, Swenson SC. 2011. Improving canopy processes in the Community Land Model version 4 (CLM4) using global flux fields empirically inferred from FLUXNET data. *Journal of Geophysical Research: Biogeosciences* **116** : G2
- Brodribb TJ, Holbrook NM . 2004 . Diurnal depression of leaf hydraulic conductance in a tropical tree species. *Plant, Cell and Environment* **27** : 820–827.
- Bunce JA. 1992. Stomatal conductance, photosynthesis and respiration of temperate deciduous tree seedlings grown outdoors at an elevated concentration of carbon dioxide. *Plant, Cell & Environment* **15** : 541–549.
- Burnett AC, Davidson K, Serbin SP, Rogers A. 2019. The 'one-point method' for estimating maximum carboxylation capacity of photosynthesis: a cautionary tale. *Plant, Cell & Environment* .**42**: 2472-2481.
- Coursolle C, Prud'Homme GO, Lamothe M, Isabel N. 2019. Measuring rapid A-C_i curves in boreal conifers: black spruce and balsam fir. *Frontiers in Plant Science* **10** : 1276
- De Kauwe MG, Lin Y-S, Wright IJ, Medlyn BE, Crous KY, Ellsworth DS, Maire V, *et al.* . 2016 . A test of the 'one-point method' for estimating maximum carboxylation capacity from field-measured, light-saturated photosynthesis. *New Phytologist* **210** : 1130–1144.
- Dodd AN, Parkinson K, Webb AAR . 2004 . Independent circadian regulation of assimilation and stomatal conductance in the *ztl-1* mutant of *Arabidopsis* . *New Phytologist* **162** : 63–70.
- Duursma RA .2015 . Plantecophys—an R package for analysing and modelling leaf gas exchange data. *PLoS ONE* **10** : e0143346.

- Epron D, Dreyer E, Bréda N . 1992 .** Photosynthesis of oak trees [*Quercus petraea* (Matt.) Liebl.] during drought under field conditions: diurnal course of net CO₂ assimilation and photochemical efficiency of photosystem II. *Plant, Cell and Environment* **15** : 809–820.
- Farquhar GD, Caemmerer S, Berry JA. 1980.** A biochemical model of photosynthetic CO₂ assimilation in leaves of C₃ species. *Planta* **149** : 78–90.
- Flexas J, Scoffoni C, Gago J, Sack L . 2013 .** Leaf mesophyll conductance and leaf hydraulic conductance: an introduction to their measurement and coordination. *Journal of Experimental Botany* **64** : 3965–3981.
- Franks PJ, Bonan GB, Berry JA, Lombardozzi DL, Holbrook NM, Herold N, Oleson KW .2018 .** Comparing optimal and empirical stomatal conductance models for application in Earth system models. *Global Change Biology* **24** : 5708–5723.
- Friedlingstein P, Meinshausen M, Arora VK, Jones CD, Anav A, Liddicoat SK, Knutti R . 2014 .** Uncertainties in CMIP5 Climate Projections due to Carbon Cycle Feedbacks. *Journal of Climate* **27** : 511–526.
- Friend AD. 2010.** Terrestrial plant production and climate change. *Journal of Experimental Botany* **61** : 1293–1309.
- Gamon JA . 2015 .** Reviews and syntheses: optical sampling of the flux tower footprint. *Biogeosciences* **12** : 4509–4523.
- Harrison MT, Kelman WM, Moore AD, Evans JR . 2010 .** Grazing winter wheat relieves plant water stress and transiently enhances photosynthesis. *Functional Plant Biology* **37** : 726–736.
- Kattge J, Knorr W. 2007.** Temperature acclimation in a biochemical model of photosynthesis: a reanalysis of data from 36 species. *Plant, Cell & Environment* **30** : 1176–1190.
- Kets K, Darbah JNT, Sober A, Riikonen J, Sober J, Karnosky DF . 2010 .** Diurnal changes in photosynthetic parameters of *Populus tremuloides* , modulated by elevated concentrations of CO₂ and/or O₃ and daily climatic variation. *Environmental Pollution* **158** : 1000–1007.
- Kobza J, Seemann JR. 1989.** Regulation of ribulose-1,5-bisphosphate carboxylase activity in response to diurnal changes in irradiance. *Plant Physiology* **89** : 918–924.
- Krinner G, Viovy N, de Noblet-Ducoudré N, Ogée J, Polcher J, Friedlingstein P, Ciais P *et al* . 2005 .** A dynamic global vegetation model for studies of the coupled atmosphere-biosphere system. *Global Biogeochemical Cycles* **19** : GB105.
- Kromdijk J, Glowacka K, Leonelli L, Gabilly ST, Iwai M, Niyogi KK, Long SP . 2016 .** Improving photosynthesis and crop productivity by accelerating recovery from photoprotection. *Science* **354** : 857–861.
- Law BE, Kelliher FM, Baldocchi DD, Anthoni PM, Irvine J, Moore D, Van Tuyl S . 2001 .** Spatial and temporal variation in respiration in a young ponderosa pine forest during a summer drought. *Agricultural and Forest Meteorology* **110** : 27–43.
- Lawrence EH, Stinziano JR, Hanson DT . 2019 .** Using the rapid A-C_i response (RAC_iR) in the Li-Cor 6400 to measure developmental gradients of photosynthetic capacity in poplar. *Plant, Cell & Environment* **42** : 740–750.
- Leakey ABD, Bernacchi CJ, Dohleman FG, Ort DR, Long SP .2004 .** Will photosynthesis of maize (*Zea mays*) in the US corn belt increase in future [CO₂] rich atmosphere? An analysis of diurnal courses of CO₂ uptake under free-air concentration enrichment (FACE). *Global Change Biology* **10** : 951–962.
- LeBauer DS, Wang D, Richter KT, Davidson CC, Dietze MC. 2013.** Facilitating feedbacks between field measurements and ecosystem models. *Ecological Monographs* **83** : 133–154.

- Le Quere C, Andrew RM, Canadell JG, Sitch S, Korsbakken JI, Peters GP, Manning AC, Boden TA, Tans PP, Houghton RA et al. 2016.** Global carbon budget 2016. *Earth Systems Science Data* **8** : 605–649.
- Leverenz JW .1981 .** Photosynthesis and transpiration in large forest-grown Douglas-fir: diurnal variation. *Canadian Journal of Botany* **59** : 349–356.
- Lin Y-S, Medlyn BE, Duursma RA, Prentice IC, Wang H, Baig S, Eamus D, et al . 2015 .** Optimal stomatal behaviour around the world. *Nature Climate Change* **5** : 459–464.
- Lindvall J, Svensson G, Hannay C . 2013 .** Evaluation of near-surface parameters in the two versions of the atmospheric model in CESM1 using flux station observations. *Journal of Climate* **26** : 26–44.
- Lombardozi DL, Smith NG, Cheng SJ, Dukes JS, Sharkey TD, Rogers A, Fisher R, Bonan GB .2018 .** Triose phosphate limitation in photosynthesis models reduces leaf photosynthesis and global terrestrial carbon storage. *Environmental Research Letters* **13** : 074025.
- Lombardozi DL, Bonan GB, Smith NG, Dukes JS, Fisher RA .2015 .** Temperature acclimation of photosynthesis and respiration: A key uncertainty in the carbon cycle-climate feedback. *Geophysical Research Letters* **42** : 8624–8631.
- Long SP, Humphries S .1994 .** Photoinhibition of photosynthesis in nature. *Annual Review of Plant Physiology and Plant Molecular Biology* **45** : 633–662.
- Lovenduski NS, Bonan GB. 2017.** Reducing uncertainty in projections of terrestrial carbon uptake. *Environmental Research Letters* **12** : 044020.
- Matthews JSA, Viallet-Chabrand SRM, Lawson T . 2017 .** Diurnal variation in gas exchange: the balance between carbon fixation and water loss. *Plant Physiology* **174** : 614–623.
- Medlyn BE, Duursma RA, Eamus D, Ellsworth DS, Prentice IC, Barton CVM, Crous KY, et al .2011 .** Reconciling the optimal and empirical approaches to modelling stomatal conductance. *Global Change Biology* **17** : 2134–2144.
- Miner GL, Bauerle WL, Baldocchi DD . 2017 .** Estimating the sensitivity of stomatal conductance to photosynthesis: a review. *Plant, Cell & Environment* **40** : 1214–1238.
- Mystakidis S, Davin EL, Gruber N, Seneviratne SI .2016 .** Constraining future terrestrial carbon cycle projections using observation-based water and carbon flux estimates. *Global Change Biology* **22** : 2198–2215.
- Nardini A, Salleo S, Andri S . 2005 .** Circadian regulation of leaf hydraulic conductance in sunflower (*Helianthus annuus* L. cv. Margot). *Plant, Cell & Environment* **28** : 750–759.
- Nascimento HCS, Marengo RA . 2013 .** Mesophyll conductance variations in response to diurnal environmental factors in *Myrcia paivae* and *Miconia guianensis* in Central Amazonia. *Photosynthetica* **51** : 457–464.
- Oleson K, Lawrence D, Bonan G, Drewniak B, Huang M, Koven C, Levis S, Li F, Riley W, Subin Z, et al. 2013 .** *Technical description of version 4.5 of the Community Land Model (CLM)* . National Center for Atmospheric Research, Boulder, CO.
- Panek J . 2004 .** Ozone uptake, water loss and carbon exchange dynamics in annually drought-stressed *Pinus ponderosa* forests: measured trends and parameters for uptake modeling. *Tree Physiology* **24** : 277–290.
- Parry MAJ, Andralojc PJ, Parmar S, Keys AJ, Habash D, Paul MJ, Alred R, Quick WP, Servaites JC. 1997.** Regulation of Rubisco by inhibitors in the light. *Plant, Cell & Environment* **20** : 528–534.

- Pérez P, Morcuende R, Martín del Molino I, Martínez-Carrasco R .2005** . Diurnal changes of Rubisco in response to elevated CO₂, temperature and nitrogen in wheat grown under temperature gradient tunnels. *Environmental & Experimental Botany* **53** : 13–27.
- Pinheiro J, Bates D, DebRoy S, Sarkar D, R Core Team .2018** . nlme: linear and nonlinear mixed effects models. R package version 3.1-137. <URL: <https://CRAN.R-project.org/package=nlme>>.
- Portis Jr. AR. 2003**. Rubisco activase - Rubisco's catalytic chaperone. *Photosynthesis Research* **75** : 11–27.
- R Core Team . 2018** . R: a language and environment for statistical computing. *R Foundation for Statistical Computing* , Vienna, Austria. R version 3.5.1. URL: <https://www.R-project.org/>.
- Resco de Dios V . 2017** . Circadian regulation and diurnal variation in gas exchange. *Plant Physiology* **175** : 3–4.
- Resco de Dios V, Gessler A, Ferrio JP, Alday JG, Bahn M, del Castillo J, Devidal S et al . 2016a** . Circadian rhythms have significant effects on leaf-to-canopy scale gas exchange under field conditions. *GigaScience* **5** : 43.
- Resco de Dios V, Loik ME, Smith R, Aspinwall MJ, Tissue DT .2016** . Genetic variation in circadian regulation of nocturnal stomatal conductance enhances carbon assimilation and growth. *Plant, Cell & Environment* **39** : 3–11.
- Resco de Dios V, Goulden ML, Ogle K, Richardson AD, Hollinger DY, Davidson EA, Alday JG et al . 2012** . Endogenous circadian regulation of carbon dioxide exchange in terrestrial ecosystems. *Global Change Biology* **18** : 1956–1970.
- Robinson SP, Portis AR. 1988**. Release of the nocturnal inhibitor, carboxyarabinitol-1-phosphate, from ribulose biphosphate carboxylase/oxygenase by Rubisco activase. *FEBS Letters***233** : 413–416.
- Rodà F, Retana J, Garcia CA, Bellot J . 1999** .*Ecology of Mediterranean evergreen oak forests* (Vol. 37). Springer Science & Business Media.
- Rogers A . 2014** . The use and misuse of V_{c,max} in Earth System Models. *Photosynthesis Research* **119** : 15–29.
- Rogers A, Medlyn BE, Dukes JS, Bonan G, von Caemmerer S, Dietze MC, Kattge J, Leakey ADB, Mercado LM, Niinemets Ü et al.2017** . A roadmap for improving the representation of photosynthesis in Earth system models. *The New Phytologist***213** : 22–42.
- Rogers A, Medlyn BE, Dukes JS. 2014**. Improving representation of photosynthesis in Earth System Models. *New Phytologist***204** :12–14.
- Rogers A, Ellsworth DS, Humphries SW. 2001**. Possible explanation of the disparity between the *in vitro* and *in vivo* measurements of Rubisco activity: a study in loblolly pine grown in elevated p CO₂. *Journal of Experimental Botany* **52** : 1555–1561.
- Ricciuto D, Sargsyan K, Thornton P . 2018** . The impact of parametric uncertainties on biogeochemistry in the E3SM land model. *Journal of Advances in Modeling Earth Systems* **10** : 297–319.
- Sack L, Buckley TN, Scoffoni C . 2016** . Why are leaves hydraulically vulnerable? *Journal of Experimental Botany***67** : 4917–4919.
- Sage RF, Way DA, Kubien DS . 2008** . Rubisco, Rubisco activase, and global climate change. *Journal of Experimental Botany* **59** : 1581–1595.
- Sage RF, Reid CD, Moore BD, Seemann JR. 1993**. Long-term kinetics of the light-dependent regulation of ribulose-1,5-bisphosphate carboxylase/oxygenase activity in plants with and without 2-carboxyarabinitol 1-phosphate. *Planta* **191** : 222–230.

- Salvucci ME, Anderson JC. 1987.** Factors affecting the activation state and the level of total activity of ribulose biphosphate carboxylase in tobacco protoplasts. *Plant Physiology* **85** : 66–71.
- Sargsyan K, Safta C, Najm HN, Debusschere BJ, Ricciuto D, Thornton P. 2014.** Dimensionality reduction for complex models via Bayesian compressive sensing. *International Journal for Uncertainty Quantification* **4** :63–93.
- Sharwood RE, Crous KY, Whitney SM, Ellsworth DS, Ghannoum O. 2017.** Linking photosynthesis and leaf N allocation under future elevated CO₂ and climate warming in *Eucalyptus globulus* . *Journal of Experimental Botany* **68** :1157–1167.
- Singsaas EL, Ort DR, DeLucia EH . 2000 .** Diurnal regulation of photosynthesis in understory saplings. *New Phytologist* **145** : 39–49.
- Sitch S, Smith B, Prentice IC, Arneth A, Bondeau A, Cramer W, Kaplan JO, Levis S, Lucht W, Sykes MT, Thonicke K, Venevsky S. 2003.** Evaluation of ecosystem dynamics, plant geography and terrestrial carbon cycling in the LPJ dynamic global vegetation model. *Global Change Biology* **9** :161–185.
- Smith NG, Malyshev SL, Shevliakova E, Kattge J, Dukes JS . 2015 .** Foliar temperature acclimation reduces simulated carbon sensitivity to climate. *Nature Climate Change* **6** : 407–411.
- Smith NG, Keenan TF, Prentice IC, Wang H, Wright IJ, Niinemets U, Crous KY, Domingues TF, Guerrieri R, Ishida FY, Kattge J, Kruger EL, Maire V, Rogers A, Serbin SP, Tarvainen L, Togashi HF, Townsend PA, Wang M, Weerasinghe LK, Zhou SX. 2019.** Global photosynthetic capacity is optimized to the environment. *Ecology Letters* **22** : 506–517.
- Stinziano JR . 2018 .** Rapid A/C_i response analysis with racir. R package version 1.0.0. *Zenodo* doi: 10.5281/zenodo.1420513. <URL: <https://github.com/jstinzi/racir>>.
- Stinziano JR, Way DA . 2017 .** Autumn photosynthetic decline and growth cessation in seedlings of white spruce are decoupled under warming and photoperiod manipulations. *Plant, Cell & Environment* **40** :1296–1316.
- Stinziano JR, Hanson DT, McDermitt DK, Lynch DJ, Saathoff AJ, Morgan PB . 2019a .** The rapid A/C_i response (RACiR): A guide to best practices. *New Phytologist* **221** : 625 - 627.
- Stinziano JR, Morgan PB, Lynch DJ, Saathoff AJ, McDermitt DK, Hanson DT . 2017 .** The rapid A/C_i response (RACiR): photosynthesis in the phenomic era. *Plant, Cell & Environment* ,**40** : 1252–1262.
- Streusand VJ, Portis AR. 1987.** Rubisco activase mediates ATP-dependent activation of ribulose biphosphate carboxylase. *Plant Physiology* **85** : 152–154.
- Sun J, Okita TW, Edwards GE . 1999 .** Modification of carbon partitioning, photosynthetic capacity, and O₂ sensitivity in *Arabidopsis* plants with low ADP-glucose pyrophosphorylase activity. *Plant Physiology* **119** : 267–276.
- Tenhunen JD, Lange OL, Gebel J, Beyschlag W, Weber JA .1984 .** Changes in photosynthetic capacity, carboxylation efficiency, and CO₂ compensation point associated with midday stomatal closure and midday depression of net CO₂ exchange of leaves of *Quercus suber* . *Planta* **162** : 193–203.
- Tholen D, Boom C, Noguchi K, Ueda S, Katase T, Terashima I. 2008.** The chloroplast avoidance response decreases internal conductance to CO₂ diffusion in *Arabidopsis thaliana* leaves. *Plant, Cell & Environment* **31** :1688–1700.
- Wolz KJ, Wertin TM, Abordo M, Wang D, Leakey ADB .2017 .** Diversity in stomatal function is integral to modelling plant carbon and water fluxes. *Nature Ecology & Evolution* **1** : 1292–1298.

Wu J, Albert LP, Lopes AP, Restrepo-Coupe N, Hayek M Wiedemann KT, Guan K, et al . 2016 . Leaf development and demography explain photosynthetic seasonality in Amazon evergreen forests. *Science* **351** : 972–976.

Wullschlegel SD . 1993 . Biochemical limitations to carbon assimilation in C₃ plants - a retrospective analysis of the A/C_i curves from 109 species. *Journal of Experimental Botany* **44** : 907–920.

Zhang N, Kallis RP, Ewy RG, Portis AR. 2002. Light modulation of Rubisco in *Arabidopsis* requires a capacity for redox regulation of the larger Rubisco activase isoform. *Proceedings of the National Academy of Sciences of the United States of America* **99** : 3330–3334.

Tables

Table 1. Leaf chamber conditions for each species for RACiR measurements.

Species	I_{sat}	VPD_{leaf}	T_{leaf}	FS	FR	$\Delta\Pi$	Rate	Range	Date
<i>Asclepias speciosa</i>	1800	2.5	30	10000	600	0.2	100	300 - 900	28/06/2018
<i>Capsicum annuum</i>	1000	1.8	25	10000	600	0.2	100	600 - 100	30/11/2016
<i>Cedrus deodar</i>	1750	2.5	30	14000	600	0.05	60	300 - 900	24/08/2018
<i>Ginkgo biloba</i>	1500	2.5	30	10000	600	0.2	100	300 - 1000	24/08/2018
<i>Malus domestica</i>	1800	1.5	25	10000	600	0.2	100	600 - 100	09/10/2016
<i>Pinus ponderosa</i>	2000	1.5	25	10000	600	0.2	70	300 - 1000	26/10/2017
<i>Populus deltoides</i>	1000	1.5	25	10000	600	0.2	100	600 - 100	31/10/2016
<i>Populus trichocarpa</i>	1000	1.5	25	10000	600	0.2	100	600 - 100	31/10/2016
<i>Quercus muehlenbergii</i>	1500	2.5	30	10000	600	0.2	100	300 - 900	28/06/2018
<i>Rosa grandiflora</i>	1000	2.5	30	10000	600	0.2	100	300 - 900	28/06/2018

RACiR: the rapid A/C_i response; I_{sat} : saturating light intensity ($\mu\text{mol m}^{-2} \text{s}^{-1}$); VPD_{leaf} : leaf to air vapor pressure deficit (kPa); T_{leaf} : leaf temperature ($^{\circ}\text{C}$); FS : fan speed (rpm); FR : flow rate ($\mu\text{mol s}^{-1}$); $\Delta\Pi$: chamber overpressure (kPa); Rate: rate of RACiR ($\mu\text{mol CO}_2 \text{mol}^{-1} \text{min}^{-1}$); Range: range of RACiR ($\mu\text{mol CO}_2 \text{mol}^{-1}$).

Table 2. Modelled net daily carbon (C) gain under scenarios of diurnally changing, peak, average, or minimum V_{cmax} and J_{max} , Percentage changes are expressed as change relative to the diurnal scenario. Bold values indicate cases where diurnal changes in photosynthetic capacity (both V_{cmax} and J_{max}) were significant.

	Daily C Gain (g C m ⁻² day ⁻¹)	Daily C Gain (g C m ⁻² day ⁻¹)	Daily C Gain (g C m ⁻² day ⁻¹)	Daily C Gain (g C m ⁻² day ⁻¹)
Species	June 28 Diurnal	June 28 Peak	June 28 Average	June 28 Minimum
<i>Asclepias speciosa</i>	3.98	4.53 14%	3.98 0.3%	2.77 -30%
<i>Capsicum annuum</i>	4.49	6.34 41%	4.7 5%	2.77 -38%
<i>Cedrus deodar</i>	4.36	7.61 75%	5.91 36%	1.15 -74%
<i>Ginkgo biloba</i>	3.1	3.8 23%	2.77 -10%	0.86 -72%
<i>Malus domestica</i>	0.86	2.7 215%	1.15 34%	0.86 0%
<i>Pinus ponderosa</i>	6.79	11.52 70%	8.08 19%	5.52 -18%

	Daily C Gain (g C m ⁻² day ⁻¹)	Daily C Gain (g C m ⁻² day ⁻¹)	Daily C Gain (g C m ⁻² day ⁻¹)	D
<i>Populus deltoides</i>	3.86	6.14	3.33	-
		59%	-14%	-
<i>Populus trichocarpa</i>	3.51	3.95	3.58	3
		13%	2%	-
<i>Quercus muehlenbergii</i>	1.72	3.55	1.74	0
		106%	1.00%	-
<i>Rosa grandiflora</i>	1.25	2.57	1.4	-
		105%	11%	1

Figure Captions

Figure 1 – Diurnal air temperature (T), photosynthetically active radiation (Q), and relative humidity (RH) used for modelling A_{net} in all species. Dates indicate the environmental conditions at the University of New Mexico in 2018. Grey regions indicate night.

Figure 2 – Diurnal variation of apparent V_{cmax} (a, b, c) and J_{max} (d, e, f) show consistent declines by the end of day at 25 °C in *Populus deltoides* (a, d; $N = 6$), *Capsicum annuum* (b, e; $N = 6$), *Malus domestica* (b, e; $N = 6$), *Populus trichocarpa* (b, e; $N = 4$) but not *Pinus ponderosa* (c, f; $N = 3$). At 30 °C there are diurnal declines in photosynthetic capacity in *Asclepias speciosa* (J_{max} only; d; $N = 6$), *Quercus muehlenbergii* (a, d; $N = 5$), *Rosa grandiflora* (b, e; $N = 6$), and *Ginkgo biloba* (c, f; $N = 3$) but not in *Cedrus deodar* (c, f; $N = 4$). Data presented as means \pm s.e.m.

Figure 3 – Apparent J_{max} is strongly correlated with apparent V_{cmax} across all species. Data presented as means for each timepoint for each species; s.e.m. was not included for clarity.

Figure 4 – Relative V_{cmax} (a-c) and J_{max} (d-f) for all species shown in Fig. 1. Data presented as means \pm s.e.m.

Figure 5 – Modelled diurnal A_{net} for *Asclepias speciosa* (a), *Capsicum annuum* (b), *Malus domestica* (c), *Quercus muehlenbergii* (d), *Populus deltoides* (e), *Populus trichocarpa* (f), *Rosa grandiflora* (g), *Ginkgo biloba* (h), *Pinus ponderosa* (i), and *Cedrus deodar* (j) under conditions of constant maximum V_{cmax} and J_{max} (Peak), and diurnally changing V_{cmax} and J_{max} (Changing), constant mean V_{cmax} and J_{max} (Average), and constant minimum V_{cmax} and J_{max} .

Figure 6 – Apparent V_{cmax} (a), J_{max} (b), and A_{net} (c) did not decline significantly after 5 one-minute clamps on the same leaf spot of individuals of *Populus deltoides*, *Capsicum annuum*, and *Populus trichocarpa*. $N = 6$, data presented as means \pm s.e.m.

Figure 7 – Modelled versus measured net CO₂ assimilation (A_{net}) (a) and stomatal conductance (g_s). Solid line indicates 1:1 relationship. See text for statistics.

Figures

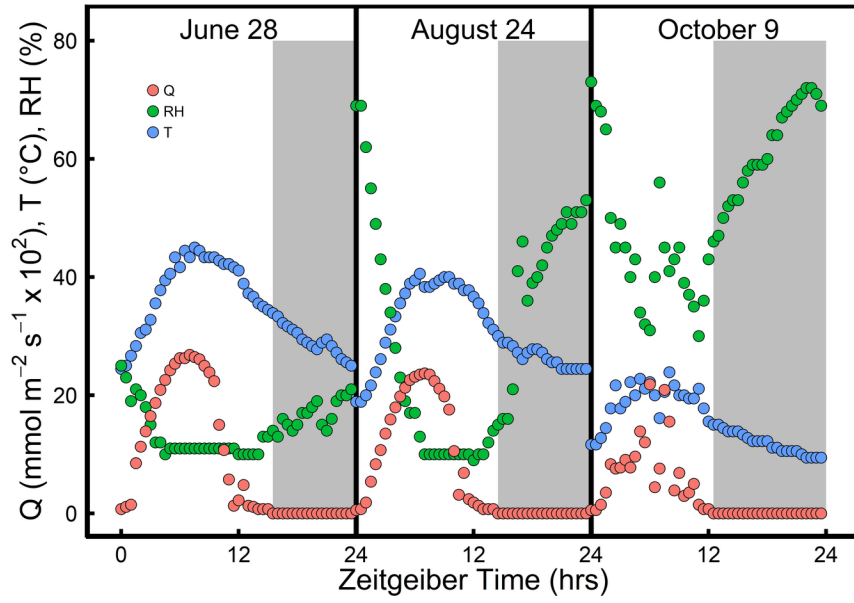


Figure 1

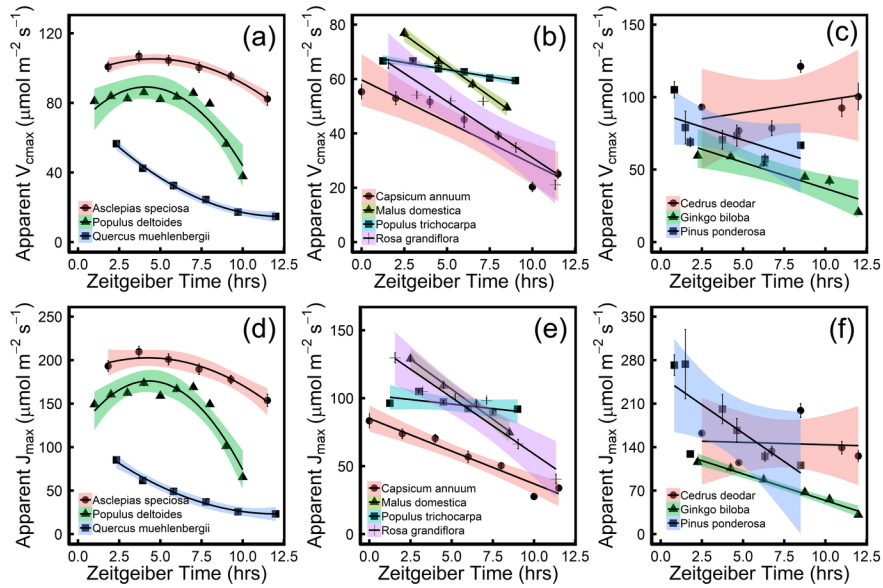


Figure 2

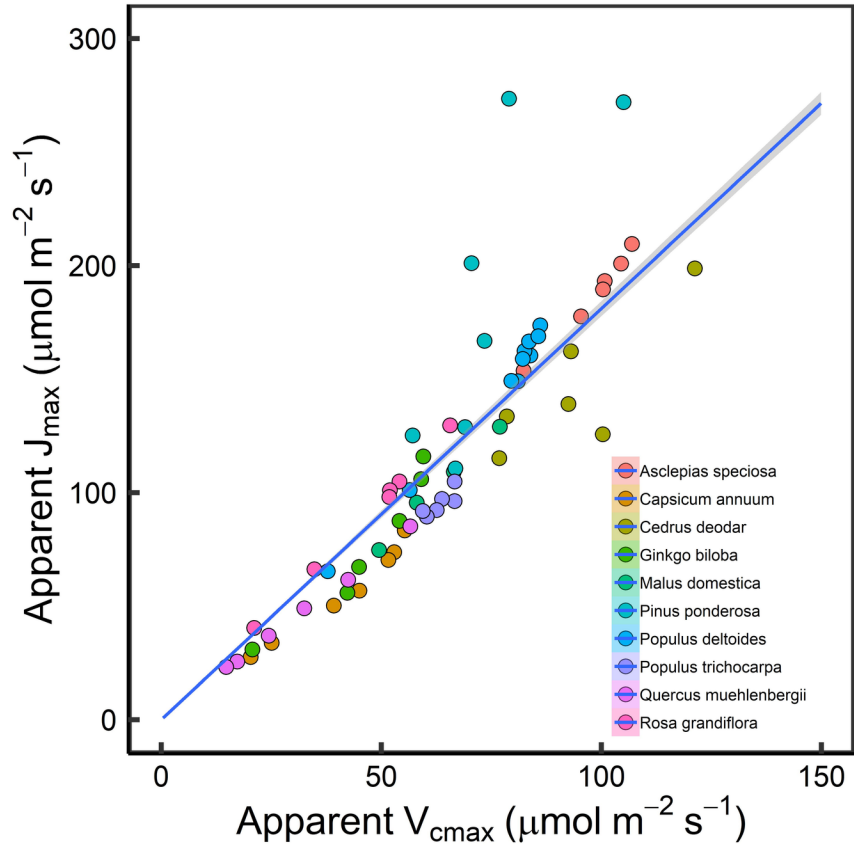


Figure 3

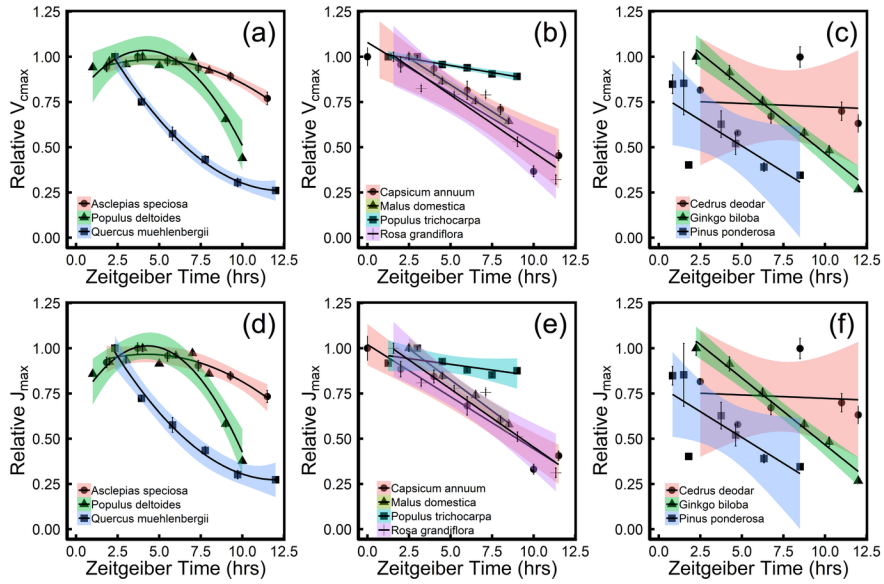


Figure 4

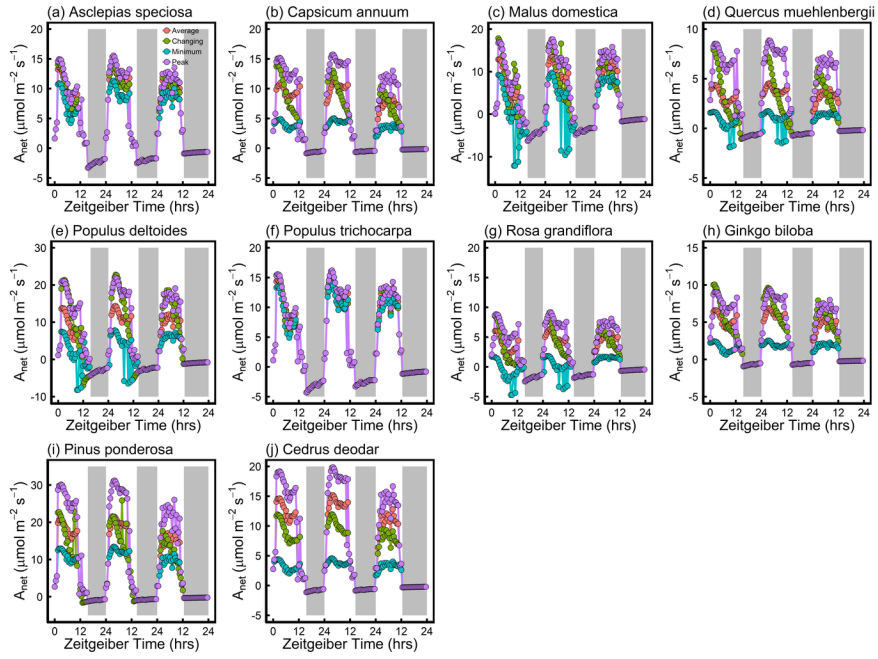


Figure 5

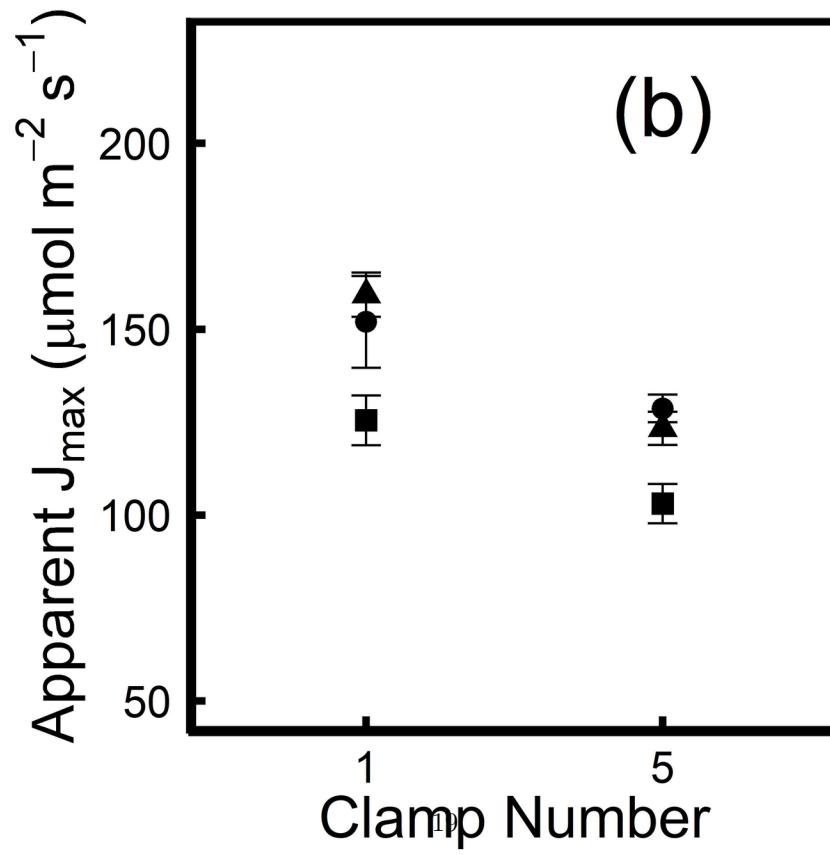
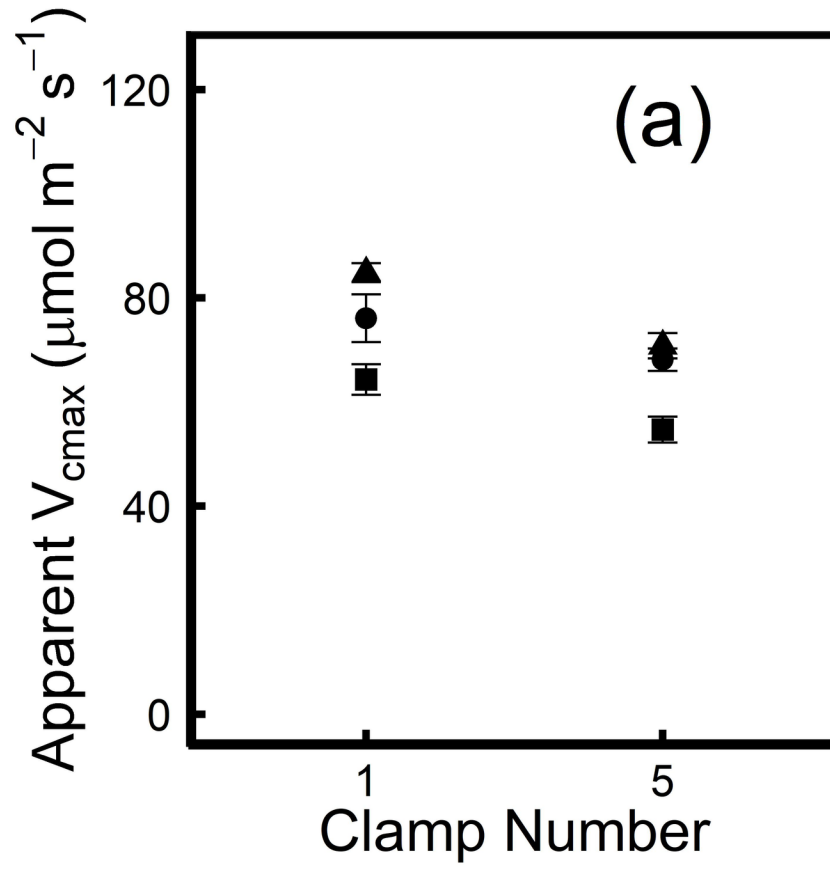


Figure 6

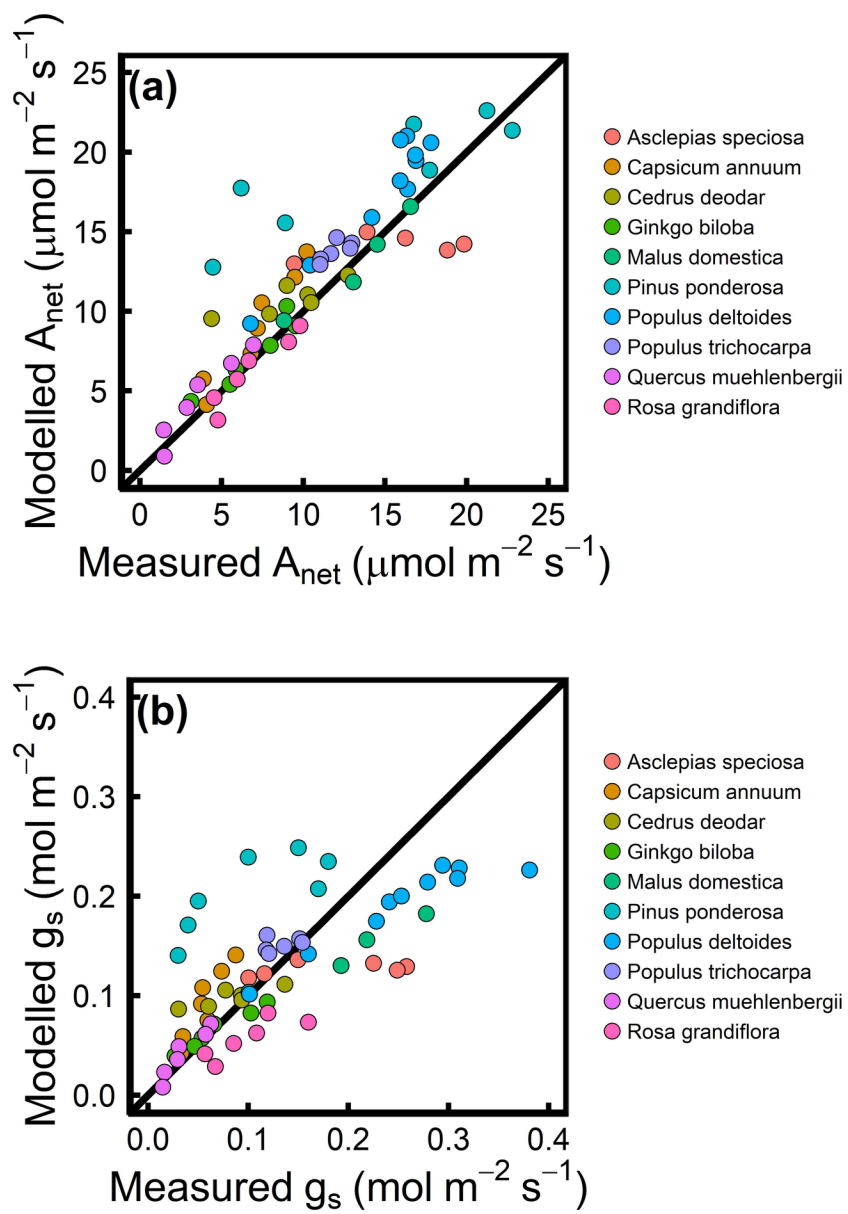


Figure 7

